

العنوان:	THE IMPACT OF COST AND FOULING ON HEAT EXCHANGER INVENTORY IN POWER AND REFRIGERATION SYSTEMS
المؤلف الرئيسي:	Qureshi, Bilal Ahmed
مؤلفين آخرين:	Sharqawy, Mostafa H., Zubair, Syed M.(co-super., super.)
التاريخ الميلادي:	2014
موقع:	الظهران
الصفحات:	1 - 240
رقم MD:	648777
نوع المحتوى:	رسائل جامعية
اللغة:	English
الدرجة العلمية:	رسالة دكتوراه
الجامعة:	جامعة الملك فهد للبترول والمعادن
الكلية:	عمادة الدراسات العليا
الدولة:	السعودية
قواعد المعلومات:	Dissertations
مواضيع:	الهندسة الميكانيكية، المخزون الحراري، التبريد
رابط:	https://search.mandumah.com/Record/648777

ABSTRACT

Name: Bilal Ahmed Qureshi

Title of Study: The Impact of Cost and Fouling on Heat Exchanger Inventory in Power and Refrigeration Systems

Major Field: Mechanical Engineering

Date of Degree: March, 2014

The first part of this study focuses on predicting the effect of variation in inventory (overall conductance) allocated on power and refrigeration systems wherein fouling, which results in decrease of this inventory, is considered as a main application. Experimental work was performed on a 1.5 ton vapor compression system which showed that system parameters and properties varied logarithmically when overall conductance was reduced. Then specific examples of power and refrigeration systems were simulated beginning with endoreversible single-stage cycles and then the Rankine and simple vapor compression cycles. Based upon these simulations and the experimental work, an equation was proposed to predict effect of reduction in overall conductance on all system properties and performance parameters using non-dimensional quantities. Agreement was found to be within 1.15% of simulated and predicted values. Such an equation helps to reduce the number of experiments and/or numerical simulations.

The second part of this study focused on thermoeconomic optimization of different power and refrigeration systems for endoreversible and irreversible cases using the allocated heat exchanger inventories. The systems investigated include a thermodynamic model of a vapor compression cycle with dedicated mechanical subcooling as well as endoreversible cases of the dedicated and integrated mechanical subcooling cycles along with an endoreversible power cycle with one feedwater heater. It was found that a practical minimum with respect to the dimensionless cost equations for the fluid to ambient high-side absolute temperature ratio existed for all cost equations. The connection between endoreversible and irreversible cycles for this ratio was shown to establish viability of the endoreversible results. Furthermore, it was found that the cost functions for simpler cycles can be derived from those of more complex systems. Also, if the only difference between a power and refrigeration cycle is that the cycle is flowing in the opposite direction, then multiplying a minus sign on one side of the cost equations of a system would provide the cost equations for the other system. Finally, a holistic view of cost optimization in power and refrigeration systems is presented, which constitutes a step forward in thermoeconomic optimization theory as it resulted in generalized cost equations.

DOCTOR OF PHILOSOPHY IN MECHANICAL ENGINEERING

KING FAHD UNIVERSITY OF PETROLEUM AND MINERALS

DHAHRAN, SAUDI ARABIA

ملخص بحث

درجة الدكتوراة في الفلسفة

الاسم : بلال أحمد قريشي

العنوان: أثر التكلفة والإفساد في مبادل حراري المخزون في الطاقة وأنظمة التبريد

التخصص : الهندسة الميكانيكية

تاريخ التخرج : مارس ٢٠١٤

يركز الجزء الأول من هذه الدراسة على تأثير الكمية (UA) والتي تعبر عن المخزون الحراري على الاتساخ في المبادلات الحرارية في محطات القوي الكهربائية وأنظمة التبريد و التي يؤدي تزايد الاتساخ فيها إلى تناقص المخزون الحراري. وقد تم اجراء دراسة معملية على وحدة تبريد سعة طن ونصف تبريد تعمل بضغط البخار حيث أوضحت الدراسة أن متغيرات التشغيل والخصائص تتغير بشكل لوغاريتمي مع تغير المخزون الحراري. وبناء على ذلك تمت محاكاة دائرة تبريد ذات أطراف مرتجة أحادية المرحلة بالإضافة إلى دائرة مبسطة تعمل بضغط البخار. وقد تم استنباط معادلة للتنبؤ بالانخفاض في المخزون الحراري وذلك من الدراسة المعملية ونتائج المحاكاة. وتقوم المعادلة المستنبطة بحساب التغير المتوقع في المخزون الحراري حسب ظروف التشغيل وخواص المواد المستخدمة بنمط لا يعتمد على نظام الوحدات المستخدم وقد تم حساب التغير في نتائج المعادلة بالمقارنة بالنتائج المعملية وكانت متوافقة حيث لا يتعدى الخطأ فيها ١,١٥%. ومن المتوقع أن تسهم هذه المعادلة في توفير الكثير من التجارب المعملية والمحاكاة في المستقبل.

وتم في الجزء الثاني من الدراسة التركيز على الوضع الأمثل على أساس مبادئ كل من الديناميكا الحرارية والاقتصاد لمختلف النظم التي تمت دراستها. واشتملت الدراسة على نموذج مبني على الديناميكا الحرارية لوحدة

تبريد تعمل بضغط البخار مزودة بنظام تبريد ميكانيكي دوني بالإضافة لمنظومة قوى حرارية مع نظام سخان المياه المغذي. وقد تبين وجود حد أدنى عملي فيما يتعلق بمعادلات التكلفة ذات نمط لا يعتمد على نظام الوحدات المستخدم لنسبة درجة حرارة السوائل المستخدمة مقسومة على درجة الحرارة المطلقة وذلك لكل المعادلات. كما تبين الصلة بين الدورات مرتجة النهايات والأخرى الغير مرتجة وعلاوة على ذلك، فقد وجد أن وظائف التكلفة للدورات والأنظمة المعقدة يمكن استخلاصها من الأنظمة البسيطة. أيضا، إذ كان الفرق الوحيد بين دورات توليد القدرة ودورات التبريد هو ان اتجاه التدفق يكون معاكسا لبعضهم البعض وبالتالي فإن ضرب علامة السالب فى جانب واحد من معادلات التكلفة من شأنه أن يوفر معادلات التكاليف للنظام الآخر. أخيرا، تم تقديم نظرة شمولية لتحسين التكلفة فى أنظمة الطاقة والتبريد، الأمر الذي يشكل خطوة إلى الأمام فى إيجاد ظروف التشغيل الأمثل حراريا واقتصاديا كما بينت الدراسة أنه يمكن تعميم معادلات التكلفة على لعديد من المنظومات.

درجة الدكتوراة فى الفلسفة فى الهندسة الميكانيكية

جامعة الملك فهد للبترول والمعادن

الظهران- المملكة العربية السعودية

العنوان:	THE IMPACT OF COST AND FOULING ON HEAT EXCHANGER INVENTORY IN POWER AND REFRIGERATION SYSTEMS
المؤلف الرئيسي:	Qureshi, Bilal Ahmed
مؤلفين آخرين:	Sharqawy, Mostafa H., Zubair, Syed M.(co-super., super.)
التاريخ الميلادي:	2014
موقع:	الظهران
الصفحات:	1 - 240
رقم MD:	648777
نوع المحتوى:	رسائل جامعية
اللغة:	English
الدرجة العلمية:	رسالة دكتوراه
الجامعة:	جامعة الملك فهد للبترول والمعادن
الكلية:	عمادة الدراسات العليا
الدولة:	السعودية
قواعد المعلومات:	Dissertations
مواضيع:	الهندسة الميكانيكية، المخزون الحراري، التبريد
رابط:	https://search.mandumah.com/Record/648777

Table of Contents

ACKNOWLEDGEMENTS	v
LIST OF TABLES	xi
LIST OF FIGURES	xii
ABSTRACT (English)	xvii
ABSTRACT (Arabic)	xix
CHAPTER 1	
INTRODUCTION	1
1.1 Motivation	1
1.2 General Background	2
1.3 Thesis Objectives	3
1.4 Inventory Reduction due to Fouling: Research Approach	4
1.5 Optimal Allocation for Cost Minimization: Research Approach.....	5
1.6 Organization	7
CHAPTER 2	
LITERATURE REVIEW	8
2.1 Optimal Allocation for Cost Minimization	8
2.2 Inventory Reduction due to Fouling.....	17
CHAPTER 3	
MATHEMATICAL MODELS	26
3.1 Curzon-Ahlborn Cycle	26
3.2 Reversed Curzon-Ahlborn Cycle	29
3.3 Simple Rankine Power Cycle.....	31
3.3.1 Description and modeling	31

3.3.2 Model validation.....	35
3.4 Simple Vapor Compression Cycle	36
3.4.1 Description and modeling	36
3.4.2 Model validation.....	41
3.5 Vapor Compression Cycle with Dedicated Mechanical Subcooling	43
3.5.1 Description and modeling	43
3.5.2 Model validation.....	48
CHAPTER 4	
VAPOR COMPRESSION SYSTEM: EXPERIMENTAL WORK.....	52
4.1 Experimental Setup and Procedure	52
4.2 Data Analysis	57
CHAPTER 5	
VAPOR COMPRESSION SYSTEM WITH DEDICATED MECHANICAL SUBCOOLING: EXPERIMENTAL AND NUMERICAL WORK.....	65
5.1 Experimental Work	65
5.1.1 Experimental setup and procedure	66
5.1.2 Data analysis.....	71
5.2 Numerical Work.....	86
CHAPTER 6	
PREDICTING EFFECT OF FOULING ON UA-DEGRADATION IN POWER AND REFRIGERATION SYSTEMS.....	92
6.1 Methodology and Procedure	92
6.2 Determining the Fouling Prediction Model.....	93
6.2.1 Observations from Curzon-Ahlborn cycle	93

6.2.2 Observations from reversed Curzon-Ahlborn cycle.....	96
6.2.3 Fouling model.....	99
6.3 Determining the Constants for the Fouling Prediction Model	101
6.3.1 Steps for deriving model constants	101
6.3.2 Buckingham Pi applied to a reversed CA cycle.....	102
6.3.3 Buckingham Pi applied to a CA cycle.....	106
6.3.4 Reversed Curzon-Ahlborn cycle	107
6.3.5 Curzon-Ahlborn cycle	113
6.3.6 Vapor compression system.....	115
6.3.7 Rankine power cycle	119
CHAPTER 7	
COST OPTIMIZATION IN POWER AND REFRIGERATION SYSTEMS.....	122
7.1 Thermoeconomic Optimization of a Vapor Compression Refrigeration System	122
7.2 Thermoeconomic Optimization for a Carnot Representation of Mechanical Subcooling Cycles.....	130
7.2.1 Constant Work Rate	137
7.2.2 Constant Cooling Rate.....	141
7.2.3 Constant Heat Rejection Rates – Both Condensers.....	144
7.2.4 Constant Heat Transfer Rate in Subcooler	147
7.3 Thermoeconomic Optimization of Mechanical Subcooling Systems using Thermodynamic Models.....	153
7.4 Thermoeconomic Optimization for a Carnot Power Cycle with one Feedwater Heater	158
7.4.1 Constant work rate.....	164

7.4.2 Constant heating rejection rate	172
7.4.3 Constant heat addition rate	173
7.4.4 Constant heat transfer rate in the feedwater heater	176
7.4.5 Effect of unit cost ratios	179
7.5 Holistic View of Thermoeconomic Optimization in Power and Refrigeration Systems.....	185
CHAPTER 8	
CONCLUSIONS AND RECOMMENDATIONS.....	190
8.1 Conclusions	190
8.1.1 Experimental Work	190
8.1.2 Predicting the effect of fouling.....	191
8.1.3 Thermoeconomic optimization.....	192
8.2 Recommendations and Future Work.....	194
8.2.1 Predicting the effect of fouling.....	194
8.2.2 Cost optimization	195
NOMENCLATURE.....	196
APPENDIX A: Calibration of Thermocouples	201
APPENDIX B: Calibration of Pressure Transducers	203
APPENDIX C: Experimental Data for SVCC	206
APPENDIX D: Experimental Data for VCC-DMS	219
APPENDIX E: Steps for Buckingham Pi Theorem.....	225
APPENDIX F: Cost Optimization Representation for VCC-DMS.....	227
APPENDIX G: VCC-IMS Cost Optimization Equation Derivation	229

REFERENCES.....	231
VITAE.....	241

LIST OF TABLES

Table 3.1:	Percentage error in calculated values for Rankine power cycle model ..36
Table 3.2:	Comparison of performance data from Stoecker and Jones [96] and current model42
Table 3.3:	Comparison of experimental data of Dopazo and Fernandez-Seara [100] and the current (modified) model50
Table 4.1:	Uncertainties in measuring devices.55
Table 4.2:	List of R^2 -values and logarithmic fit equations for plotted lines in Figs. 4.3-4.6.64
Table 5.1:	Average percentage increase in second-law efficiency.88
Table 5.2:	Average uncertainty calculated for plotted quantities.88
Table 6.1:	Selected variables in terms of MLtT and FLtT system for reversed CA cycle103
Table 6.2:	Summary of dimensionless Pi groups for determining fouling constants.....104
Table 6.3:	Selected variables in terms of MLtT and FLtT system for CA cycle...106
Table 7.1:	Comparison of θ_{min} in SVCC and endoreversible case [$\eta_c = 1$]128
Table 7.2:	Comparison of θ_{min} in SVCC and endoreversible case [$\eta_c = 0.65$]129

LIST OF FIGURES

Figure 1.1.	Schematic of a dedicated mechanical subcooling system	6
Figure 2.1.	Various fouling models	19
Figure 3.1.	Temperature - specific entropy plot for a heat transfer-limited power cycle with finite capacitance rate source and sink temperatures	27
Figure 3.2.	Temperature - specific entropy plot for a heat transfer-limited refrigeration cycle with finite capacitance rate source and sink temperatures	30
Figure 3.3.	Schematic of a simple Rankine cycle	33
Figure 3.4.	Schematic of a simple vapor compression cycle	37
Figure 3.5.	Pressure - enthalpy diagram of a refrigeration cycle with dedicated sub-cooling	44
Figure 4.1(a).	Experimental plant	54
Figure 4.1(b).	Schematic of a vapor compression cycle	54
Figure 4.2.	Experimental plant with partially blocked condenser	56
Figure 4.3.	Variation of normalized compressor power with percentage increase in condenser blockage	60
Figure 4.4.	Variation of normalized COP with percentage increase in condenser blockage	61
Figure 4.5.	Variation of normalized condenser pressure with percentage increase in condenser blockage	61
Figure 4.6.	Variation of normalized superheat temperature at compressor exit with percentage increase in condenser blockage	62
Figure 4.7(a).	Logarithmic fitting of normalized power consumption for data of Federov [104]	63
Figure 4.7(b).	Logarithmic fitting of normalized superheat temperature at compressor exit for data of current work	63
Figure 5.1.	Experimental plant	67
Figure 5.2(a).	Schematic of a vapor compression cycle with dedicated mechanical sub-cooling	68
Figure 5.2(b).	Pressure-enthalpy diagram of a refrigeration cycle with dedicated sub-cooling	69
Figure 5.3(a).	Variation of compressor discharge temperature – Base configuration	74

Figure 5.3(b).	Variation of ambient temperature – Base configuration.....	75
Figure 5.4(a).	Variation of discharge pressure – Base configuration.....	75
Figure 5.4(b).	Variation of suction pressure – Base configuration.....	76
Figure 5.5.	Variation of cooling capacity and compressor power requirement – Base configuration.....	76
Figure 5.6.	Variation of COP – Base configuration.....	77
Figure 5.7(a).	Variation of compressor discharge temperatures – Subcooler configuration.....	78
Figure 5.7(b).	Variation of ambient temperature – Subcooler configuration.....	78
Figure 5.8(a).	Variation of main cycle discharge pressure – Subcooler configuration.....	79
Figure 5.8(b).	Variation of main cycle suction pressure – Subcooler configuration.....	79
Figure 5.9(a).	Variation of small cycle discharge pressure – Subcooler configuration.....	80
Figure 5.9(b).	Variation of small cycle suction pressure – Subcooler configuration.....	80
Figure 5.10(a).	Variation of compressor power (Main cycle) - Subcooler configuration.....	81
Figure 5.10(b).	Variation of compressor power (Small cycle) – Subcooler configuration.....	81
Figure 5.11(a).	Variation in amount of subcooling – Subcooler configuration.....	83
Figure 5.11(b).	Variation in subcooler effectiveness – Subcooler configuration.....	83
Figure 5.11(c).	Variation in subcooler power – Subcooler configuration.....	84
Figure 5.12(a).	Variation in cooling capacity – Subcooler configuration.....	84
Figure 5.12(b).	Variation in COP – Subcooler configuration.....	85
Figure 5.13.	Comparison of second-law efficiency variation for both configurations.....	87
Figure 5.14.	Percentage change in second-law efficiency due to use of subcooling.....	87
Figure 5.15(a).	Effect of equal UA degradation (in both condensers and the main evaporator) on main cycle – for R134a _m - R134a _{sc} , R410A _{sc} , R407C _{sc}	90
Figure 5.15(b).	Effect of equal UA degradation (in both condensers and the main evaporator) on dedicated sub-cooler section – for R134a _m - R134a _{sc} , R410A _{sc} , R407C _{sc}	91
Figure 6.1(a).	Effect of reduction in boiler conductance only: CA cycle.....	94
Figure 6.1(b).	Effect of reduction in condenser conductance only: CA cycle.....	94
Figure 6.1(c).	Effect of reduction in (equal) condenser and boiler conductance: CA cycle.....	95
Figure 6.2(a).	Effect of reduction in condenser conductance only: Reversed CA cycle.....	97

Figure 6.2(b).	Effect of reduction in evaporator conductance only: Reversed CA cycle.....	97
Figure 6.2(c).	Effect of reduction in (equal) condenser and evaporator conductance: Reversed CA cycle.....	98
Figure 6.3(a).	Determining fouling data constants for T_{cd} variation for Case 1 (for $C_r=0.7$): ER.....	109
Figure 6.3(b).	Determining fouling data constants for T_{cd} variation for Case 2 (for $C_r=0.7$): ER.....	109
Figure 6.4(a).	Determining fouling data constants for T_{cd} variation for Case 1 (for $C_r=1$): SVCC.....	116
Figure 6.4(b).	Determining fouling data constants for T_{cd} variation Case 2 (for $C_r=1$): SVCC.....	116
Figure 6.5(a).	Determining fouling data constants for \dot{m}_{sl} variation for Case 1 (for $C_r=0.04$): RPC.....	120
Figure 6.5(b).	Determining fouling data constants for \dot{m}_{sl} variation Case 2 (for $C_r=0.04$): RPC.....	120
Figure 7.1.	Effect of compressor efficiency on cost function F_2	124
Figure 7.2.	θ versus the cost function F_1 from Antar and Zubair [26].....	124
Figure 7.3.	Variation of cost function F_1 with respect to θ [$\eta_c = 0.65$]: SVCC.....	126
Figure 7.4.	Variation of cost function F_1 with respect to θ [$\eta_c = 1$]: SVCC.....	126
Figure 7.5.	Variation of cost function F_2 with respect to θ [$\eta_c = 0.65$]: SVCC.....	127
Figure 7.6.	Variation of cost function F_2 with respect to θ [$\eta_c = 1$]: SVCC.....	127
Figure 7.7.	Total conductance versus the unit cost ratio for a SVCC with specified cooling capacity.....	129
Figure 7.8.	T-s diagram of Carnot representation of dedicated subcooling system.....	131
Figure 7.9(a).	Dimensionless HEICE for constant work rate vs. θ : Effect of varying Φ_1	140
Figure 7.9(b).	Dimensionless HEICE for constant work rate vs. θ : Effect of varying K	140
Figure 7.10(a).	Dimensionless HEICE for constant cooling rate vs. Φ_1 : Effect of varying θ_1	143
Figure 7.10(b).	Dimensionless HEICE for constant cooling rate vs. Φ_2 : Effect of varying θ_1	143
Figure 7.11.	Dimensionless HEICE for constant cooling rate vs. θ_1 : Effect of varying Φ_1	145

Figure 7.12.	Dimensionless HEICE for heat transfer rate in the subcooler vs. Φ_2 : Effect of varying θ_1	149
Figure 7.13(a).	Schematic of an integrated mechanical subcooling system	151
Figure 7.13(b).	Integrated Carnot cycle with subcooler	151
Figure 7.14.	Effect of main compressor efficiency on cost function F_2	155
Figure 7.15.	Variation of cost function F_1 with respect to θ_1 [$\eta_c = 0.65$]: VCC- DMS	155
Figure 7.16.	Variation of cost function F_1 with respect to θ_1 [$\eta_c = 1$]: VCC-DMS ..	156
Figure 7.17.	Variation of cost function F_2 with respect to θ_1 [$\eta_c = 0.65$]: VCC- DMS	156
Figure 7.18.	Variation of cost function F_2 with respect to θ_1 [$\eta_c = 1$]: VCC-DMS ..	157
Figure 7.19(a).	Schematic of an endoreversible power cycle with an open feedwater heater	159
Figure 7.19(b).	T-s diagram of an endoreversible power cycle with one open feedwater heater	159
Figure 7.20(a).	Dimensionless HEICE for constant work rate vs. Φ_1 : Effect of varying ξ	167
Figure 7.20(b).	Dimensionless HEICE for constant work rate vs. Φ_1 : Effect of varying θ_1	167
Figure 7.20(c).	Dimensionless HEICE for constant work rate vs. Φ_1 : Effect of varying Φ_2	168
Figure 7.21(a).	Dimensionless HEICE for constant work rate vs. θ_1 : Effect of varying ξ	170
Figure 7.21(b).	Dimensionless HEICE for constant work rate vs. θ_1 : Effect of varying Φ_1	170
Figure 7.21(c).	Dimensionless HEICE for constant work rate vs. θ_1 : Effect of varying Φ_2	171
Figure 7.22(a).	Dimensionless HEICE for constant heat rejection rate vs. θ_1 : Effect of varying ξ	174
Figure 7.22(b).	Dimensionless HEICE for constant heat rejection rate vs. θ_1 : Effect of varying Φ_1	174
Figure 7.22(c).	Dimensionless HEICE for constant heat rejection rate vs. θ_1 : Effect of varying Φ_2	175
Figure 7.23(a).	Dimensionless HEICE for constant heat addition rate vs. θ_1 : Effect of varying ξ	177

Figure 7.23(b).	Dimensionless HEICE for constant heat addition rate vs. θ_1 : Effect of varying Φ_1	177
Figure 7.23(c).	Dimensionless HEICE for constant heat addition rate vs. θ_1 : Effect of varying Φ_2	178
Figure 7.24(a).	Dimensionless HEICE for constant heat transfer rate in the feedwater heater vs. θ_1 : Effect of varying ξ	180
Figure 7.24(b).	Dimensionless HEICE for constant heat transfer rate in the feedwater heater vs. θ_1 : Effect of varying Φ_1	180
Figure 7.24(c).	Dimensionless HEICE for constant heat transfer rate in the feedwater heater vs. θ_1 : Effect of varying Φ_2	181
Figure 7.25(a).	Example of all conductances versus unit cost ratio of cold to hot end at $G_{OFH} = 1$	183
Figure 7.25(b).	Example of all conductances versus unit cost ratio of cold to hot end at $G_{OFH} = 0.5$	183
Figure 7.25(c).	Example of all conductances versus unit cost ratio of cold to hot end at $G_{OFH} = 0.1$	184
Figure 7.26.	Holistic view of thermoeconomic optimization	187
Figure A.1.	Calibration curve of thermocouples.....	202
Figure B.1.	Calibration curve of pressure transducer #1	204
Figure B.2.	Calibration curve of pressure transducer #2	204
Figure B.3.	Calibration curve of pressure transducer #3	205
Figure B.4.	Calibration curve of pressure transducer #4	205
Figure F.1.	Dedicated Carnot cycle with subcooler - Alternative	228

العنوان:	THE IMPACT OF COST AND FOULING ON HEAT EXCHANGER INVENTORY IN POWER AND REFRIGERATION SYSTEMS
المؤلف الرئيسي:	Qureshi, Bilal Ahmed
مؤلفين آخرين:	Sharqawy, Mostafa H., Zubair, Syed M.(co-super., super.)
التاريخ الميلادي:	2014
موقع:	الظهران
الصفحات:	1 - 240
رقم MD:	648777
نوع المحتوى:	رسائل جامعية
اللغة:	English
الدرجة العلمية:	رسالة دكتوراه
الجامعة:	جامعة الملك فهد للبترول والمعادن
الكلية:	عمادة الدراسات العليا
الدولة:	السعودية
قواعد المعلومات:	Dissertations
مواضيع:	الهندسة الميكانيكية، المخزون الحراري، التبريد
رابط:	https://search.mandumah.com/Record/648777

**THE IMPACT OF COST AND FOULING ON HEAT EXCHANGER
INVENTORY IN POWER AND REFRIGERATION SYSTEMS**

BY

BILAL AHMED QURESHI

A Dissertation Presented to the
DEANSHIP OF GRADUATE STUDIES

KING FAHD UNIVERSITY OF PETROLEUM & MINERALS

DHAHRAN, SAUDI ARABIA

1963 ١٣٨٣

In Partial Fulfillment of the
Requirements for the Degree of

DOCTOR OF PHILOSOPHY

In

MECHANICAL ENGINEERING

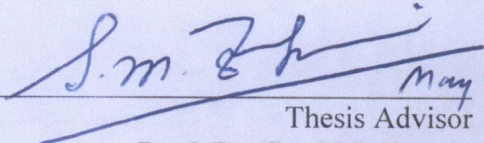
MARCH 2014

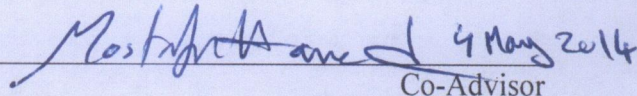
**KING FAHD UNIVERSITY OF PETROLEUM & MINERALS
DHAHRAN, SAUDI ARABIA**

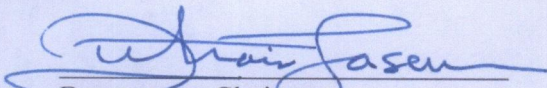
DEANSHIP OF GRADUATE STUDIES

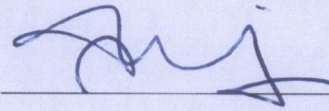
This dissertation, written by **Bilal Ahmed Qureshi** under the direction of his dissertation advisor and approved by his dissertation committee, has been presented to and accepted by the Dean of Graduate Studies, in partial fulfillment of the requirements for the degree of **DOCTOR OF PHILOSOPHY** in *Mechanical Engineering*.

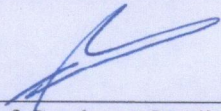
Dissertation Committee

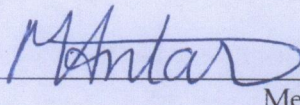

May 4, 2014
Thesis Advisor
Prof. Dr. Syed M. Zubair


4 May 2014
Co-Advisor
Dr. Mostafa H. Sharqawy


Department Chairman
Dr. Zuhair M. Gasem

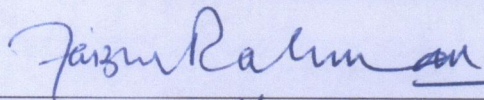

4 / May / 2014
Member
Prof. Dr. Shahzada Z. Shuja


Dean of Graduate Studies
Dr. Salam A. Zummo


May 4, 2014
Member
Prof. Dr. Mohamed A. Antar

20/5/14
Date




4-May-2014 Member
Dr. Faizur Rahman

©Bilal Ahmed Qureshi

2014

This work is dedicated to my wife and children.

ACKNOWLEDGEMENTS

All praises and thanks are due to Allah (subhaanahu wa ta'aala) for bestowing me with knowledge, health and patience to complete this work. After that, acknowledgement is due to KFUPM and NSTIP (project # 08-ENE50-4) for the support given to this research project through its funding and excellent facilities.

I acknowledge, with deep gratitude and appreciation, the inspiration, encouragement, valuable time and continuous guidance given to me by my Committee Chairman, Dr. Syed M. Zubair. Secondly, I am grateful to my Committee Co-Chairman, Dr. Mostafa H. Sharqawy and Committee members Dr. Mohamed A. Antar, Dr. S. Z. Shuja and Dr. Faizur Rahman for their constructive guidance and technical support. Thanks are also due to the Department secretaries, Mr. Qamar Zaman, Mr. Jaleel and Mr. Lateef for their help and assistance. Special thanks are due to Mr. Syed Younus Ahmed and Mr. Peter Varghese for their continued technical support for the experimental work.

My heart-felt gratitude to my wife and children for the sacrifices they made. Also, my sincerest appreciation for the support and encouragement from my parents, my wife's parents and my brothers. I would also like to thank my friends Usama Siddiqui, Haris Malik, Usman Kaleem, Ameer Hamza, Osama Hasan, Khalid and all others who provided wonderful company and good memories that will last a life time.

Table of Contents

ACKNOWLEDGEMENTS	v
LIST OF TABLES	xi
LIST OF FIGURES	xii
ABSTRACT (English)	xvii
ABSTRACT (Arabic)	xix
CHAPTER 1	
INTRODUCTION	1
1.1 Motivation	1
1.2 General Background	2
1.3 Thesis Objectives	3
1.4 Inventory Reduction due to Fouling: Research Approach	4
1.5 Optimal Allocation for Cost Minimization: Research Approach.....	5
1.6 Organization	7
CHAPTER 2	
LITERATURE REVIEW	8
2.1 Optimal Allocation for Cost Minimization	8
2.2 Inventory Reduction due to Fouling.....	17
CHAPTER 3	
MATHEMATICAL MODELS	26
3.1 Curzon-Ahlborn Cycle	26
3.2 Reversed Curzon-Ahlborn Cycle	29
3.3 Simple Rankine Power Cycle.....	31
3.3.1 Description and modeling	31

3.3.2 Model validation.....	35
3.4 Simple Vapor Compression Cycle	36
3.4.1 Description and modeling	36
3.4.2 Model validation.....	41
3.5 Vapor Compression Cycle with Dedicated Mechanical Subcooling	43
3.5.1 Description and modeling	43
3.5.2 Model validation.....	48
CHAPTER 4	
VAPOR COMPRESSION SYSTEM: EXPERIMENTAL WORK.....	52
4.1 Experimental Setup and Procedure	52
4.2 Data Analysis	57
CHAPTER 5	
VAPOR COMPRESSION SYSTEM WITH DEDICATED MECHANICAL SUBCOOLING: EXPERIMENTAL AND NUMERICAL WORK.....	65
5.1 Experimental Work	65
5.1.1 Experimental setup and procedure	66
5.1.2 Data analysis.....	71
5.2 Numerical Work.....	86
CHAPTER 6	
PREDICTING EFFECT OF FOULING ON UA-DEGRADATION IN POWER AND REFRIGERATION SYSTEMS.....	92
6.1 Methodology and Procedure	92
6.2 Determining the Fouling Prediction Model.....	93
6.2.1 Observations from Curzon-Ahlborn cycle	93

6.2.2 Observations from reversed Curzon-Ahlborn cycle.....	96
6.2.3 Fouling model.....	99
6.3 Determining the Constants for the Fouling Prediction Model	101
6.3.1 Steps for deriving model constants	101
6.3.2 Buckingham Pi applied to a reversed CA cycle.....	102
6.3.3 Buckingham Pi applied to a CA cycle.....	106
6.3.4 Reversed Curzon-Ahlborn cycle	107
6.3.5 Curzon-Ahlborn cycle	113
6.3.6 Vapor compression system.....	115
6.3.7 Rankine power cycle	119
CHAPTER 7	
COST OPTIMIZATION IN POWER AND REFRIGERATION SYSTEMS.....	122
7.1 Thermoeconomic Optimization of a Vapor Compression Refrigeration System	122
7.2 Thermoeconomic Optimization for a Carnot Representation of Mechanical Subcooling Cycles.....	130
7.2.1 Constant Work Rate	137
7.2.2 Constant Cooling Rate.....	141
7.2.3 Constant Heat Rejection Rates – Both Condensers.....	144
7.2.4 Constant Heat Transfer Rate in Subcooler	147
7.3 Thermoeconomic Optimization of Mechanical Subcooling Systems using Thermodynamic Models.....	153
7.4 Thermoeconomic Optimization for a Carnot Power Cycle with one Feedwater Heater	158
7.4.1 Constant work rate.....	164

7.4.2 Constant heating rejection rate	172
7.4.3 Constant heat addition rate	173
7.4.4 Constant heat transfer rate in the feedwater heater	176
7.4.5 Effect of unit cost ratios	179
7.5 Holistic View of Thermoeconomic Optimization in Power and Refrigeration Systems.....	185
CHAPTER 8	
CONCLUSIONS AND RECOMMENDATIONS.....	190
8.1 Conclusions	190
8.1.1 Experimental Work	190
8.1.2 Predicting the effect of fouling.....	191
8.1.3 Thermoeconomic optimization.....	192
8.2 Recommendations and Future Work.....	194
8.2.1 Predicting the effect of fouling.....	194
8.2.2 Cost optimization	195
NOMENCLATURE.....	196
APPENDIX A: Calibration of Thermocouples	201
APPENDIX B: Calibration of Pressure Transducers	203
APPENDIX C: Experimental Data for SVCC	206
APPENDIX D: Experimental Data for VCC-DMS	219
APPENDIX E: Steps for Buckingham Pi Theorem.....	225
APPENDIX F: Cost Optimization Representation for VCC-DMS.....	227
APPENDIX G: VCC-IMS Cost Optimization Equation Derivation	229

REFERENCES.....	231
VITAE.....	241

LIST OF TABLES

Table 3.1:	Percentage error in calculated values for Rankine power cycle model ..	36
Table 3.2:	Comparison of performance data from Stoecker and Jones [96] and current model	42
Table 3.3:	Comparison of experimental data of Dopazo and Fernandez-Seara [100] and the current (modified) model	50
Table 4.1:	Uncertainties in measuring devices.	55
Table 4.2:	List of R^2 -values and logarithmic fit equations for plotted lines in Figs. 4.3-4.6.	64
Table 5.1:	Average percentage increase in second-law efficiency.	88
Table 5.2:	Average uncertainty calculated for plotted quantities.	88
Table 6.1:	Selected variables in terms of MLtT and FLtT system for reversed CA cycle	103
Table 6.2:	Summary of dimensionless Pi groups for determining fouling constants.....	104
Table 6.3:	Selected variables in terms of MLtT and FLtT system for CA cycle ...	106
Table 7.1:	Comparison of θ_{min} in SVCC and endoreversible case [$\eta_c = 1$]	128
Table 7.2:	Comparison of θ_{min} in SVCC and endoreversible case [$\eta_c = 0.65$]	129

LIST OF FIGURES

Figure 1.1.	Schematic of a dedicated mechanical subcooling system	6
Figure 2.1.	Various fouling models	19
Figure 3.1.	Temperature - specific entropy plot for a heat transfer-limited power cycle with finite capacitance rate source and sink temperatures	27
Figure 3.2.	Temperature - specific entropy plot for a heat transfer-limited refrigeration cycle with finite capacitance rate source and sink temperatures	30
Figure 3.3.	Schematic of a simple Rankine cycle	33
Figure 3.4.	Schematic of a simple vapor compression cycle	37
Figure 3.5.	Pressure - enthalpy diagram of a refrigeration cycle with dedicated sub-cooling	44
Figure 4.1(a).	Experimental plant	54
Figure 4.1(b).	Schematic of a vapor compression cycle	54
Figure 4.2.	Experimental plant with partially blocked condenser	56
Figure 4.3.	Variation of normalized compressor power with percentage increase in condenser blockage	60
Figure 4.4.	Variation of normalized COP with percentage increase in condenser blockage	61
Figure 4.5.	Variation of normalized condenser pressure with percentage increase in condenser blockage	61
Figure 4.6.	Variation of normalized superheat temperature at compressor exit with percentage increase in condenser blockage	62
Figure 4.7(a).	Logarithmic fitting of normalized power consumption for data of Federov [104]	63
Figure 4.7(b).	Logarithmic fitting of normalized superheat temperature at compressor exit for data of current work	63
Figure 5.1.	Experimental plant	67
Figure 5.2(a).	Schematic of a vapor compression cycle with dedicated mechanical sub-cooling	68
Figure 5.2(b).	Pressure-enthalpy diagram of a refrigeration cycle with dedicated sub-cooling	69
Figure 5.3(a).	Variation of compressor discharge temperature – Base configuration	74

Figure 5.3(b).	Variation of ambient temperature – Base configuration.....	75
Figure 5.4(a).	Variation of discharge pressure – Base configuration.....	75
Figure 5.4(b).	Variation of suction pressure – Base configuration.....	76
Figure 5.5.	Variation of cooling capacity and compressor power requirement – Base configuration.....	76
Figure 5.6.	Variation of COP – Base configuration.....	77
Figure 5.7(a).	Variation of compressor discharge temperatures – Subcooler configuration.....	78
Figure 5.7(b).	Variation of ambient temperature – Subcooler configuration.....	78
Figure 5.8(a).	Variation of main cycle discharge pressure – Subcooler configuration.....	79
Figure 5.8(b).	Variation of main cycle suction pressure – Subcooler configuration.....	79
Figure 5.9(a).	Variation of small cycle discharge pressure – Subcooler configuration.....	80
Figure 5.9(b).	Variation of small cycle suction pressure – Subcooler configuration.....	80
Figure 5.10(a).	Variation of compressor power (Main cycle) - Subcooler configuration.....	81
Figure 5.10(b).	Variation of compressor power (Small cycle) – Subcooler configuration.....	81
Figure 5.11(a).	Variation in amount of subcooling – Subcooler configuration.....	83
Figure 5.11(b).	Variation in subcooler effectiveness – Subcooler configuration.....	83
Figure 5.11(c).	Variation in subcooler power – Subcooler configuration.....	84
Figure 5.12(a).	Variation in cooling capacity – Subcooler configuration.....	84
Figure 5.12(b).	Variation in COP – Subcooler configuration.....	85
Figure 5.13.	Comparison of second-law efficiency variation for both configurations.....	87
Figure 5.14.	Percentage change in second-law efficiency due to use of subcooling.....	87
Figure 5.15(a).	Effect of equal UA degradation (in both condensers and the main evaporator) on main cycle – for R134a _m - R134a _{sc} , R410A _{sc} , R407C _{sc}	90
Figure 5.15(b).	Effect of equal UA degradation (in both condensers and the main evaporator) on dedicated sub-cooler section – for R134a _m - R134a _{sc} , R410A _{sc} , R407C _{sc}	91
Figure 6.1(a).	Effect of reduction in boiler conductance only: CA cycle.....	94
Figure 6.1(b).	Effect of reduction in condenser conductance only: CA cycle.....	94
Figure 6.1(c).	Effect of reduction in (equal) condenser and boiler conductance: CA cycle.....	95
Figure 6.2(a).	Effect of reduction in condenser conductance only: Reversed CA cycle.....	97

Figure 6.2(b).	Effect of reduction in evaporator conductance only: Reversed CA cycle.....	97
Figure 6.2(c).	Effect of reduction in (equal) condenser and evaporator conductance: Reversed CA cycle.....	98
Figure 6.3(a).	Determining fouling data constants for T_{cd} variation for Case 1 (for $C_r=0.7$): ER.....	109
Figure 6.3(b).	Determining fouling data constants for T_{cd} variation for Case 2 (for $C_r=0.7$): ER.....	109
Figure 6.4(a).	Determining fouling data constants for T_{cd} variation for Case 1 (for $C_r=1$): SVCC.....	116
Figure 6.4(b).	Determining fouling data constants for T_{cd} variation Case 2 (for $C_r=1$): SVCC.....	116
Figure 6.5(a).	Determining fouling data constants for \dot{m}_{sl} variation for Case 1 (for $C_r=0.04$): RPC.....	120
Figure 6.5(b).	Determining fouling data constants for \dot{m}_{sl} variation Case 2 (for $C_r=0.04$): RPC.....	120
Figure 7.1.	Effect of compressor efficiency on cost function F_2	124
Figure 7.2.	θ versus the cost function F_1 from Antar and Zubair [26].....	124
Figure 7.3.	Variation of cost function F_1 with respect to θ [$\eta_c = 0.65$]: SVCC.....	126
Figure 7.4.	Variation of cost function F_1 with respect to θ [$\eta_c = 1$]: SVCC.....	126
Figure 7.5.	Variation of cost function F_2 with respect to θ [$\eta_c = 0.65$]: SVCC.....	127
Figure 7.6.	Variation of cost function F_2 with respect to θ [$\eta_c = 1$]: SVCC.....	127
Figure 7.7.	Total conductance versus the unit cost ratio for a SVCC with specified cooling capacity.....	129
Figure 7.8.	T-s diagram of Carnot representation of dedicated subcooling system.....	131
Figure 7.9(a).	Dimensionless HEICE for constant work rate vs. θ : Effect of varying Φ_1	140
Figure 7.9(b).	Dimensionless HEICE for constant work rate vs. θ : Effect of varying K	140
Figure 7.10(a).	Dimensionless HEICE for constant cooling rate vs. Φ_1 : Effect of varying θ_1	143
Figure 7.10(b).	Dimensionless HEICE for constant cooling rate vs. Φ_2 : Effect of varying θ_1	143
Figure 7.11.	Dimensionless HEICE for constant cooling rate vs. θ_1 : Effect of varying Φ_1	145

Figure 7.12.	Dimensionless HEICE for heat transfer rate in the subcooler vs. Φ_2 : Effect of varying θ_1	149
Figure 7.13(a).	Schematic of an integrated mechanical subcooling system	151
Figure 7.13(b).	Integrated Carnot cycle with subcooler	151
Figure 7.14.	Effect of main compressor efficiency on cost function F_2	155
Figure 7.15.	Variation of cost function F_1 with respect to θ_1 [$\eta_c = 0.65$]: VCC- DMS	155
Figure 7.16.	Variation of cost function F_1 with respect to θ_1 [$\eta_c = 1$]: VCC-DMS ..	156
Figure 7.17.	Variation of cost function F_2 with respect to θ_1 [$\eta_c = 0.65$]: VCC- DMS	156
Figure 7.18.	Variation of cost function F_2 with respect to θ_1 [$\eta_c = 1$]: VCC-DMS ..	157
Figure 7.19(a).	Schematic of an endoreversible power cycle with an open feedwater heater	159
Figure 7.19(b).	T-s diagram of an endoreversible power cycle with one open feedwater heater	159
Figure 7.20(a).	Dimensionless HEICE for constant work rate vs. Φ_1 : Effect of varying ξ	167
Figure 7.20(b).	Dimensionless HEICE for constant work rate vs. Φ_1 : Effect of varying θ_1	167
Figure 7.20(c).	Dimensionless HEICE for constant work rate vs. Φ_1 : Effect of varying Φ_2	168
Figure 7.21(a).	Dimensionless HEICE for constant work rate vs. θ_1 : Effect of varying ξ	170
Figure 7.21(b).	Dimensionless HEICE for constant work rate vs. θ_1 : Effect of varying Φ_1	170
Figure 7.21(c).	Dimensionless HEICE for constant work rate vs. θ_1 : Effect of varying Φ_2	171
Figure 7.22(a).	Dimensionless HEICE for constant heat rejection rate vs. θ_1 : Effect of varying ξ	174
Figure 7.22(b).	Dimensionless HEICE for constant heat rejection rate vs. θ_1 : Effect of varying Φ_1	174
Figure 7.22(c).	Dimensionless HEICE for constant heat rejection rate vs. θ_1 : Effect of varying Φ_2	175
Figure 7.23(a).	Dimensionless HEICE for constant heat addition rate vs. θ_1 : Effect of varying ξ	177

Figure 7.23(b).	Dimensionless HEICE for constant heat addition rate vs. θ_1 : Effect of varying Φ_1	177
Figure 7.23(c).	Dimensionless HEICE for constant heat addition rate vs. θ_1 : Effect of varying Φ_2	178
Figure 7.24(a).	Dimensionless HEICE for constant heat transfer rate in the feedwater heater vs. θ_1 : Effect of varying ξ	180
Figure 7.24(b).	Dimensionless HEICE for constant heat transfer rate in the feedwater heater vs. θ_1 : Effect of varying Φ_1	180
Figure 7.24(c).	Dimensionless HEICE for constant heat transfer rate in the feedwater heater vs. θ_1 : Effect of varying Φ_2	181
Figure 7.25(a).	Example of all conductances versus unit cost ratio of cold to hot end at $G_{OFH} = 1$	183
Figure 7.25(b).	Example of all conductances versus unit cost ratio of cold to hot end at $G_{OFH} = 0.5$	183
Figure 7.25(c).	Example of all conductances versus unit cost ratio of cold to hot end at $G_{OFH} = 0.1$	184
Figure 7.26.	Holistic view of thermoeconomic optimization	187
Figure A.1.	Calibration curve of thermocouples	202
Figure B.1.	Calibration curve of pressure transducer #1	204
Figure B.2.	Calibration curve of pressure transducer #2	204
Figure B.3.	Calibration curve of pressure transducer #3	205
Figure B.4.	Calibration curve of pressure transducer #4	205
Figure F.1.	Dedicated Carnot cycle with subcooler - Alternative	228

ABSTRACT

Name: Bilal Ahmed Qureshi

Title of Study: The Impact of Cost and Fouling on Heat Exchanger Inventory in Power and Refrigeration Systems

Major Field: Mechanical Engineering

Date of Degree: March, 2014

The first part of this study focuses on predicting the effect of variation in inventory (overall conductance) allocated on power and refrigeration systems wherein fouling, which results in decrease of this inventory, is considered as a main application. Experimental work was performed on a 1.5 ton vapor compression system which showed that system parameters and properties varied logarithmically when overall conductance was reduced. Then specific examples of power and refrigeration systems were simulated beginning with endoreversible single-stage cycles and then the Rankine and simple vapor compression cycles. Based upon these simulations and the experimental work, an equation was proposed to predict effect of reduction in overall conductance on all system properties and performance parameters using non-dimensional quantities. Agreement was found to be within 1.15% of simulated and predicted values. Such an equation helps to reduce the number of experiments and/or numerical simulations.

The second part of this study focused on thermoeconomic optimization of different power and refrigeration systems for endoreversible and irreversible cases using the allocated heat exchanger inventories. The systems investigated include a thermodynamic model of a vapor compression cycle with dedicated mechanical subcooling as well as endoreversible cases of the dedicated and integrated mechanical subcooling cycles along with an endoreversible power cycle with one feedwater heater. It was found that a practical minimum with respect to the dimensionless cost equations for the fluid to ambient high-side absolute temperature ratio existed for all cost equations. The connection between endoreversible and irreversible cycles for this ratio was shown to establish viability of the endoreversible results. Furthermore, it was found that the cost functions for simpler cycles can be derived from those of more complex systems. Also, if the only difference between a power and refrigeration cycle is that the cycle is flowing in the opposite direction, then multiplying a minus sign on one side of the cost equations of a system would provide the cost equations for the other system. Finally, a holistic view of cost optimization in power and refrigeration systems is presented, which constitutes a step forward in thermoeconomic optimization theory as it resulted in generalized cost equations.

DOCTOR OF PHILOSOPHY IN MECHANICAL ENGINEERING

KING FAHD UNIVERSITY OF PETROLEUM AND MINERALS

DHAHRAN, SAUDI ARABIA

ملخص بحث

درجة الدكتوراة في الفلسفة

الاسم : بلال أحمد قريشي

العنوان: أثر التكلفة والإفساد في مبادل حراري المخزون في الطاقة وأنظمة التبريد

التخصص : الهندسة الميكانيكية

تاريخ التخرج : مارس ٢٠١٤

يركز الجزء الأول من هذه الدراسة على تأثير الكمية (UA) والتي تعبر عن المخزون الحراري على الاتساخ في المبادلات الحرارية في محطات القوي الكهربائية وأنظمة التبريد و التي يؤدي تزايد الاتساخ فيها إلى تناقص المخزون الحراري. وقد تم اجراء دراسة معملية على وحدة تبريد سعة طن ونصف تبريد تعمل بضغط البخار حيث أوضحت الدراسة أن متغيرات التشغيل والخصائص تتغير بشكل لوغاريتمي مع تغير المخزون الحراري. وبناء على ذلك تمت محاكاة دائرة تبريد ذات أطراف مرتجة أحادية المرحلة بالإضافة إلى دائرة مبسطة تعمل بضغط البخار. وقد تم استنباط معادلة للتنبؤ بالانخفاض في المخزون الحراري وذلك من الدراسة المعملية ونتائج المحاكاة. وتقوم المعادلة المستنبطة بحساب التغير المتوقع في المخزون الحراري حسب ظروف التشغيل وخواص المواد المستخدمة بنمط لا يعتمد على نظام الوحدات المستخدم وقد تم حساب التغير في نتائج المعادلة بالمقارنة بالنتائج المعملية وكانت متوافقة حيث لا يتعدى الخطأ فيها ١,١٥%. ومن المتوقع أن تسهم هذه المعادلة في توفير الكثير من التجارب المعملية والمحاكاة في المستقبل.

وتم في الجزء الثاني من الدراسة التركيز على الوضع الأمثل على أساس مبادئ كل من الديناميكا الحرارية والاقتصاد لمختلف النظم التي تمت دراستها. واشتملت الدراسة على نموذج مبني على الديناميكا الحرارية لوحدة

تبريد تعمل بضغط البخار مزودة بنظام تبريد ميكانيكي دوني بالإضافة لمنظومة قوى حرارية مع نظام سخان المياه المغذي. وقد تبين وجود حد أدنى عملي فيما يتعلق بمعادلات التكلفة ذات نمط لا يعتمد على نظام الوحدات المستخدم لنسبة درجة حرارة السوائل المستخدمة مقسومة على درجة الحرارة المطلقة وذلك لكل المعادلات. كما تبين الصلة بين الدورات مرتجة النهايات والأخرى الغير مرتجة وعلاوة على ذلك، فقد وجد أن وظائف التكلفة للدورات والأنظمة المعقدة يمكن استخلاصها من الأنظمة البسيطة. أيضا، إذ كان الفرق الوحيد بين دورات توليد القدرة ودورات التبريد هو ان اتجاه التدفق يكون معاكسا لبعضهم البعض وبالتالي فإن ضرب علامة السالب فى جانب واحد من معادلات التكلفة من شأنه أن يوفر معادلات التكاليف للنظام الآخر. أخيرا، تم تقديم نظرة شمولية لتحسين التكلفة فى أنظمة الطاقة والتبريد، الأمر الذي يشكل خطوة إلى الأمام فى إيجاد ظروف التشغيل الأمثل حراريا واقتصاديا كما بينت الدراسة أنه يمكن تعميم معادلات التكلفة على لعديد من المنظومات.

درجة الدكتوراة فى الفلسفة فى الهندسة الميكانيكية

جامعة الملك فهد للبترول والمعادن

الظهران- المملكة العربية السعودية

CHAPTER 1

INTRODUCTION

In this chapter, the main points of discussion will be the motivation, objectives and method of solution of this research work.

1.1 Motivation

Heat exchanger inventory is an expensive commodity. The effects of its allocation, reduction during operation (due to fouling) as well as optimizing the heat exchanger inventory of these cycles has been a subject of much discussion. Conductances are not unlimited in availability and thus have a certain dollar value attached to them that must be distributed wisely. This entails not only distribution with consideration of best performance but also of lowest cost. Thermoeconomics is a known method for this type of optimization. Furthermore, experimental and numerical work related to fouling consumes time and money. If a mathematical model can be presented that can help to

predict necessary parameters of the system, this can help to reduce the number of experiments and numerical simulations.

1.2 General Background

The heat exchanger inventory is defined as the sum of the conductances of the condenser and evaporator in a power or refrigeration cycle. One of the cornerstones of sustainable development is the cost-effective fuel saving of systems that use or produce useful energy. This, in turn, calls for more intensive and extensive system analysis while the system is still in its design phase. Such analysis has to be multi-disciplinary. Accessing the analysis from the discipline of thermodynamics is the advantage of thermoeconomics. Thermoeconomics was first developed during the sixties. The name was coined by professor M. Tribus [1]. Development of thermoeconomics to handle energy-intensive systems in general was initiated by R. Gaggioli [2-3]. In the last 25 years, the development of thermoeconomics has been impressive. Works related to endoreversible thermoeconomics by De Vos [4-5] constitutes one approach.

Where there are heat exchangers, fouling will often inevitably follow. Fouling studies are performed to ascertain the effect on performance parameters so that contingency plans can be adopted for times of failure or clean up schedules drawn up to avoid the former. Heat exchangers are one of the main components of these systems. Therefore, even a small performance degradation, due to fouling, has the potential to cause further energy consumption and/or decrease cooling capacity along with the

efficiency. This results in higher costs of running the equipment. Foulants vary in nature from mold compounds, human hair and textile fibers to airborne particulate matter and dust [6] but they all result in an overall decrease in the ability of the heat exchanger to transfer heat. Heat exchanger design is based on best practice values and experience related to fouling resistance. Experimental and numerical studies on fouling, when done correctly, often take a great amount of time and incur high costs. Reducing the number of experiments, thus, becomes a matter of great interest as this will result in saving of both time and money.

1.3 Thesis Objectives

The overall objective of this thesis dissertation is to examine the impact of fouling and cost-based optimization on both power and refrigeration systems. In this regard, the following specific objectives are proposed:

- To investigate a model, applicable to both power and refrigeration systems, that can predict the effect of reduction in conductance (UA), due to fouling, on these systems.
- Application of the proposed performance degradation model on vapor compression and power cycles using thermodynamic models.
- Experimental evaluation of the performance characteristics of a vapor compression cycle, under fouled conditions.

- Thermoeconomic optimization using a thermodynamic model for a vapor compression refrigeration system.
- Thermoeconomic optimization for a Carnot representation of a mechanical subcooling system.
- Thermoeconomic optimization of a vapor compression cycle with mechanical subcooling using a thermodynamic model.

1.4 Inventory Reduction due to Fouling: Research Approach

The first objective mentioned is to develop a model to predict effect of fouling resulting in UA-degradation on all system (properties and performance) parameters. A model will be presented that is to be used to connect three types of cases: 1) Fouling in the HX on high temperature-side only, 2) Fouling in the HX on low temperature-side only, and 3) Fouling (equally) in the HX on both high and low-temperature-side. The UA-value, which represents the conductance affected due to fouling, will be decreased from 0 to 50% to simulate the three cases mentioned. Using these simulations, an attempt will be made to develop a relationship between these three types of cases. Once this is achieved, thermodynamic models of both power and refrigeration cycles will be simulated to ascertain practical applicability of the proposed model.

Experimental evaluation of the performance characteristics of a vapor compression cycle, under fouled conditions, will also be done. For this purpose, a 1.5 ton